Korean Chem. Eng. Res., 56(2), 1-9 (2018)
https://doi.org/10.9713/kcer.2017.56.2.1
PISSN 0304-128X, EISSN 2233-9558

Hydrodynamic and Heat Transfer Studies in Riser System for Waste Heat Recovery using Chalcopyrite

Ashok Kumar Popuri*,,† and Prabhakar Garimella***

**Department of Chemical Engineering, S.V.U. College of Engineering, S.V. University, Tirupati, 517502, India*
***VFSTR University, Vadlamudi, 522202, India*
(Received 15 June 2017; Received in revised form 21 November 2017; accepted 29 November 2017)

Abstract – Energy, a critical input, is to be efficiently managed via waste heat recovery and energy reuse for the economic viability of a process industry. In particular, cement manufacture demands a huge quantum of energy, for the necessary reactions. Huge amounts of hot effluent gases are generated. Energy recovery from these waste gases is an area that is of contemporary research interest. Now, about 75% of total heat recovery takes place in the riser of the suspension pre-heater system. This article deals with the hydrodynamic and heat transfer aspects of riser typically used in the cement industry. An experimental apparatus was designed and fabricated with provision for the measurement of gas pressure and solid temperatures at different heights of the riser. The system studied was air - chalcopyrite taken in different particle sizes. Acceleration length (L_A) determined at different parametric levels was fitted to an empirical correlation: $L_A/d_t = 4.91902(d_p/d_t)^{0.10058}(w_s/w_g)^{-0.11691}(u_g\mu_g/d_t^2 g\rho_g)^{0.28574}(\rho_p/\rho_g)^{0.42484}$. An empirical model was developed for Nusselt number as a function of Reynolds and Prandtl numbers using regression analysis: $Nu = 0.40969\ (Re_p)^{0.99953}\ (Pr)^{0.03569}$.

Key words: Riser, Acceleration length, Suspension preheater, Chalcopyrite, Gas velocity

1. Introduction

The process industry is an energy intensive activity and its success and economic viability depends heavily on energy management. This realization prompts consideration of energy recovery and reuse at process conceptualization and design stage itself. Petroleum refining, petrochemicals, cement, power and several others are identified as those consuming large quantity of energy [1]. The cement industry, in particular, demands considerable energy inputs for endothermic reactions like clinker formation [2,3]. During the initial phases, the Indian cement industry employed petroleum-based products as the fuel until the oil crunch of 1973 forced them to look for alternatives [4,5]. Coal due to its easy availability has become the source of energy since then [6]. Several technological advancements, mainly aimed at reduction in energy use, have been implemented in the last fifty years [7]. Early kilns of 300-600 tpd capacity gave way to 1200 tpd units and thereafter to 3000 tpd plants [8]. The specific energy consumption decreased in the process, from 6300 kJ/kg clinker in long wet kilns to 4600 units in long dry process [9]. In semi-dry kilns, this has further gone down to 4100 units and finally, with the introduction of suspension pre-heater (SP) system coupled with pre-calcinator, the specific energy requirement is currently ~ 3350 kJ/kg clinker [10,11].

In the modern cement industry, waste heat recovery involves the use of four to five cyclones, placed one above the other and interconnected by long vertical gas ducts. Raw cement mix (limestone, clay and bauxite) is introduced into the transporting duct leading to the first stage cyclone (top most) and is preheated in suspended state, by uprising hot gas leaving the second cyclone [12]. This constitutes the first stage of waste heat recovery, hot effluent gas passing on part of its energy to the solids. Preheated suspension enters the first cyclone, where solids are separated from the gas stream. Partially heated particles move down the line, enter the interconnecting gas duct between the second and third stages, facilitating further heating of solids by the hot gas ascending from the third stage. This way, the solids get preheated to the desired temperature by exhaust gases, resulting in high heat recovery from the kiln gas. This arrangement is known as suspension pre-heater system (SP) [13,14].

Blasetti and De Lasa (2001) studied the heat transfer between the gas and solid phases in the riser section of a cyclone suspension preheater system, and suggested that the heat-transfer coefficient in the system depended on both the concentration of solid particles and the particle Reynolds number in the riser section [15-17].

Kaczmarzyk and Bandrowski (1980) postulated that the suspended solid particles were free to have other types of motion like rotational motion, in addition to axial motion, thereby causing considerable disturbance in the relatively stable laminar film adjacent to the particle surface. Consequently, there was turbulence over a larger portion of the particle surface than would have otherwise been possible with stationary particles [18,19]. The data collected for vertical pneumatic transport of granular materials was used to arrive at a correla-

† To whom correspondence should be addressed.
E-mail: ashok_kumar_popuri@yahoo.com
This is an Open-Access article distributed under the terms of the Creative Commons Attribution Non-Commercial License (http://creativecommons.org/licenses/by-nc/3.0) which permits unrestricted non-commercial use, distribution, and reproduction in any medium, provided the original work is properly cited.

tion - Nusselt number, $Nu = 0.00114\ b^{-0.5984}\ Re_p^{\ 0.8159}$ ($0.00025 < b < 0.05$ and $180 < Re_p < 1800$).

Sharlovskaya (1958) suggested a generalized equation based on the data on heat transfer between solid and fluid. The correlation was simple, in that only the Nusselt number was plotted against the Reynolds number [20].

Watanabe et al. (1991) studied experimentally the characteristics of interfacial heat transfer between gas and solid particles in the fast-fluidized bed regime, which is similar to the present heat transfer studies in many respects [21,22]. The heat transfer coefficients were estimated on the basis of temperature profiles obtained experimentally. It was stated that the particle hold-up, the velocity and the temperature distribution with in a particle influence the magnitude of heat transfer coefficient. The heat transfer coefficient was observed to increase with an increase in the suspension density. The data were found to be valid over a wide range of gas velocity and particle mass flux. Again, the heat transfer coefficient was found to decrease significantly as the riser height (measured from the bottom) is increased. It was concluded that the minimum height required for heat transfer to become stable ranged from 0.83 to 1.52 m for circulating fluidized bed systems.

2. Experimental Aspects

Studies on hydrodynamic behavior and heat transfer characteristics of the riser were carried out using cold (pressure measurement) and hot model (temperature measurement) experimental apparatus.

2-1. Experimental apparatus

Schematic diagram and fabricated experimental apparatus are shown in Figures 1 and 2. The apparatus essentially consists of a vertical transport duct, A (diameter: 0.0508 m; height: 2.1082 m); cyclone separator, B (diameter: 0.127 m; cylindrical height: 0.1778 m; conical height: 0.254 m; inlet diameter: 0.0508 m; solid outlet pipe diameter: 0.0508 m; gas outlet pipe diameter: 0.0508 m); solid storage tank, C (diameter: 0.127 m; cylindrical height: 0.4064 m; conical height: 0.2794 m); stand pipe, D (height: 0.3048 m: diameter: 0.0254 m); solid feeding line, E (diameter: 0.03175 m; length: 0.6096 m); bend, F (diameter: 0.0508 m; total flat length: 0.3048 m); orifice meter, G (diameter: 0.019 m); blower, H (2.2 kw, 3.0 hp, 415V, 3 phase induction motor, 2830 RPM, 50Hz, 4.61A, 55 IP, 150 m^3/hr, rectangular outlet: 0.0889 m x 0.0762 m); solid collection pot, I (diameter: 0.0508 m; height: 0.3048 m); auxiliary air inlet, J (diameter: 0.0254 m; length: 1.524 m); electric furnace, K (length: 0.381 m; breadth: 0.4064; height: 1.524 m; each coil height: 1.016 m; number of coils: 12); all made up of steel.

A screw conveyor transports the solid from solid storage tank to the bottom of the riser and an auxiliary air flow is also provided, to ensure smooth flow of solid particles, by preventing choking in the transport line. An orifice meter connected across pressure taps (P_1 and P_2) measures the velocity of entering air. Eighteen pressure taps (P_3 - P_{20}), each installed 0.1016 meters apart, facilitate measurement of static pressures along the height of the riser. Seven valves, each 0.3048 meters apart, are installed on the riser to permit collection of solid samples at various heights. Ten thermocouples, each 0.2032 meters apart, are also installed along the riser to measure air temperature at various heights. All the external metal surfaces are completely covered with half-an- inch thick glass wool layer, wrapped with a quarter-inch rope and finally coated with plaster of paris to prevent heat loss from the riser and to ensure near-adiabatic operation.

2-2. Experimental procedure

2-2-1. Hydrodynamic studies

Chalcopyrite particles of known size are loaded into the storage tank and the rotary valve is adjusted for a specific solid feed rate. Air from the blower is metered and is sent through the bottom of the riser to transport the solids vertically upward. The gas – solid suspension on reaching the top of the riser is separated in the cyclone separator, the solids completing their cycle along the down comer and reaching the storage vessel. Provision has been made for the collection of solid samples at various riser heights. The static pressures along the riser height are measured with the help of water manometers after the system reaches steady state. Differential pressure can be found across any section of the riser. The pressure drop across the cyclone is also measured. Experimental data are collected by varying the size of particles, the solid feed rate and the air velocity.

2-2-2. Heat transfer studies

Chalcopyrite of predetermined size is charged into the storage tank and the rotary valve is positioned for a specific solid feed rate. Air from the blower is preheated to the desired temperature in the electric furnace. As the hot air moves upwards, the solid is fed into the riser, the test section behaving like a direct contact, vertical parallel flow heat exchanger. Air velocity is so maintained as to ensure pneumatic transport of the solid particles. Heat transfer takes place between the hot air and the solid. Temperatures of air and also of solid at various riser heights are recorded. At steady state, solid samples are collected from various points into stand-by calorimeters. Final temperatures attained by the mercury thermometers in the calorimeters are recorded to obtain the temperature profile of solid within the riser. In this manner data on variations in air and particle temperatures are recorded at different air velocities, different particle sizes and different temperatures of the incoming hot air.

3. Results and Discussion

3-1. Hydrodynamic studies - acceleration (or mixing) length

Starting from the introduction of solid into the duct, various forces act upon the particles. Depending upon the mode of injection, the particle can either be at zero or negligible velocity at the bottom of the riser, after which it is accelerated at the expense of the kinetic

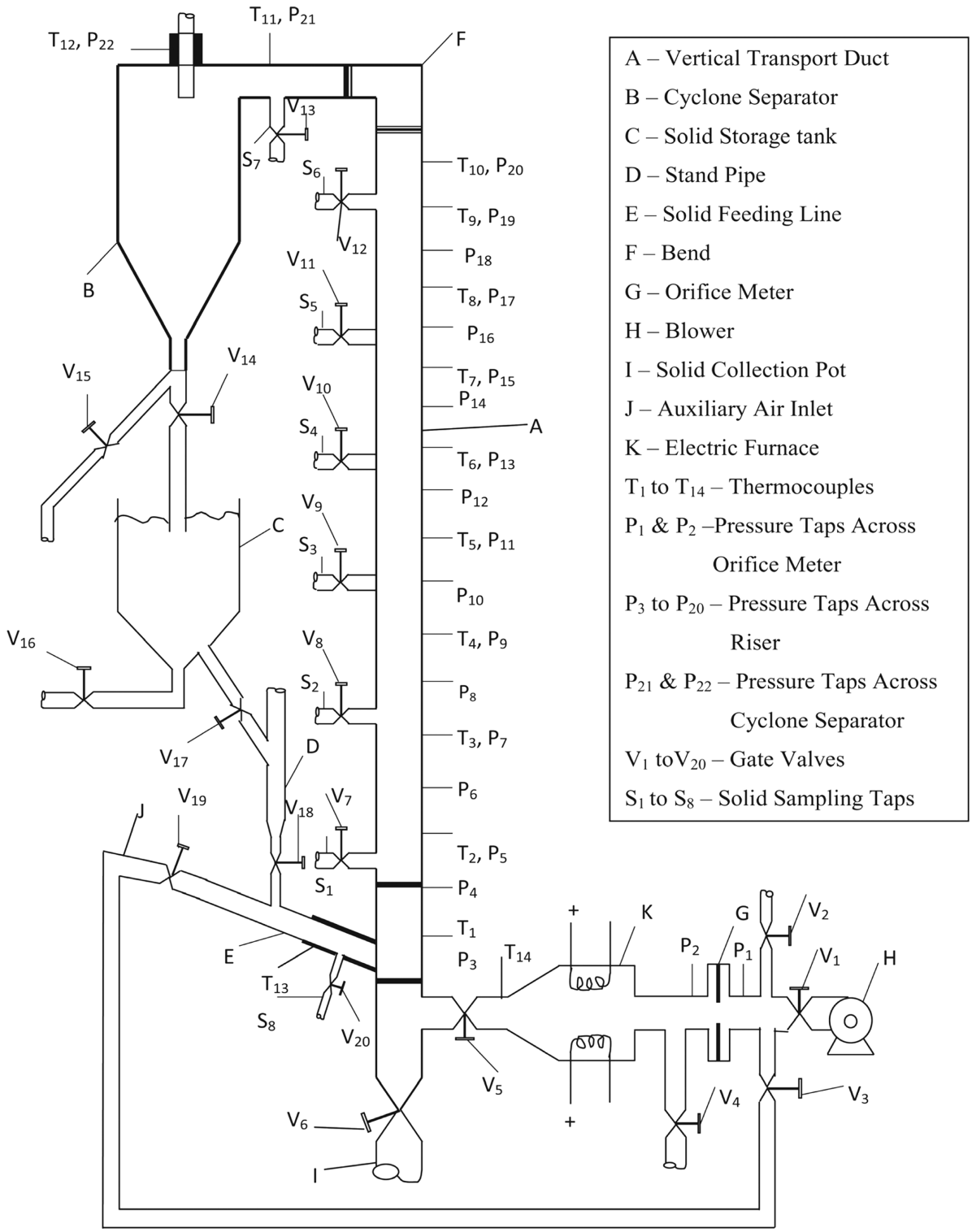

Fig. 1. Schematic diagram of experimental apparatus.

energy of the fluid. At a certain riser height, the particle velocity reaches a maximum value, which evidently depends on the system conditions. Once this velocity is reached, the system behaves like a homogeneous (dispersed) gas-solid suspension. This minimum length (or height) required for attaining a steady homogeneous flow, is termed as "Acceleration Length", L_A or "Entry Length" or "Mixing Length".

By plotting static pressure distribution against the riser height, an asymptotic trend is observed. A cross plot of riser height against pressure drop per unit length (or height) indicates a plateau, the pres-

Fig. 2. Fabricated experimental apparatus.

sure drop per unit length remaining substantially constant with riser height. This particular length (or height) is identified as the riser height, beyond which a homogeneous suspension flow occurs. Values of pressure gradient DP/DL at different riser heights are found as per the equation,

$$[\Delta P/\Delta L]_{i\,to\,(i+1)} = [DP_{(i+1)\,to\,0} - DP_{i\,to\,0}] / [L_{i+1\,\mathrm{to}\,0} - L_{i\,to\,0}] \quad (1)$$

3-1-1. Effect of gas velocity on acceleration length

Pressure gradients at different riser heights, obtained at different gas velocities, for chalcopyrite-air system, are shown in Fig. 3.

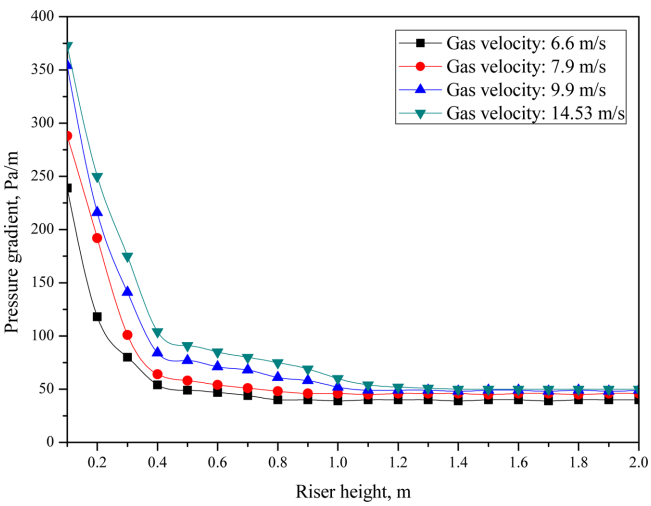

Fig. 3. Variation of pressure gradient with gas velocity (Particle size: 98 mm; Solid feed rate: 0.012 kg/sec).

Table 1. Variation of acceleration length with gas velocity

Gas velocity (u_g), m/s	Acceleration length (L_A), m
6.6	0.83
7.9	0.92
9.9	1.11
14.53	1.42

Acceleration lengths evaluated from this data are tabulated as Table 1.

Pressure gradient, which seemed to be inversely related to the riser height initially, continued to show the same trend of decrease with increase in height, but at a lower slope before reaching constancy in the ordinate level for all the three velocities studied. Pressure gradient is higher at higher gas velocities. Accordingly, acceleration length exhibited a direct dependence on the gas superficial velocity, increasing with increasing gas velocity, as indicated by the data shown in Table 1. As the gas travels past the solid, some of its kinetic energy is passed on to the solid, helping the particles to pick up speed, i.e., particles are accelerated with a simultaneous drop in the gas velocity. The higher the gap between gas and particle velocities, the more the length would be, to reach the steady flow rate. So acceleration lengths increase as the gas velocity increases.

3-1-2. Effect of particle size on acceleration length

Pressures are measured at different riser heights with different sizes of the solid particles and the resulting plots of pressure gradient vs. riser height are shown as Fig. 4 for the chalcopyrite-air system. Variation of acceleration length with particle size is given in Table 2.

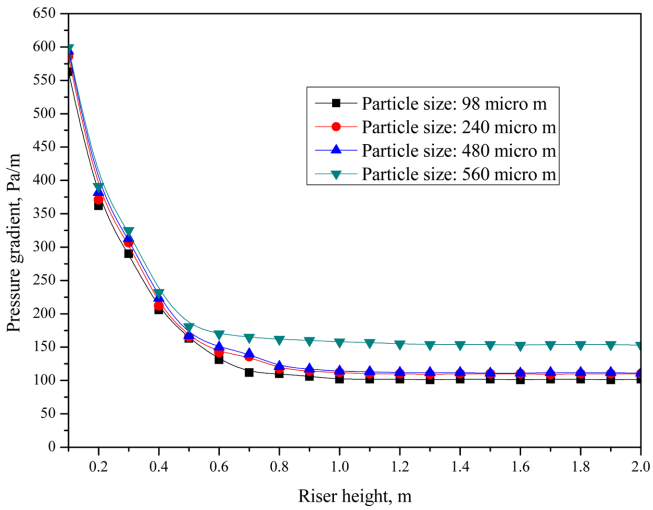

Fig. 4. Variation of pressure gradient with particle size (Gas velocity: 14.53 m/s; Solid feed rate: 0.0362 kg/sec).

Table 2. Variation of acceleration length with particle size

Particle size (d_P), μm	Acceleration length (L_A), m
98	1.03
240	1.11
480	1.19
560	1.23

Pressure decreases as the particles move up, with the smallest particle causing the highest pressure drop. Pressure drop decreases with increasing particle size at all riser heights. Packing density and particle density are the two factors that are responsible for gas pressure drop. While both are significant in case of small particles, the first factor diminishes as particle size is increased. Pressure gradient reached a steady value at a riser height of 0.7 m for all particle sizes. As far as acceleration length is concerned, higher particle size demands higher acceleration length, indicating the difficulty in accelerating bigger particles to a velocity equal to the gas velocity, overcoming the forces of gravity and drag.

3-1-3. Effect of Solid Feed Rate on Acceleration Length

Solid feed rate is the next variable studied with pressure measurement carried out at different riser heights for chalcopyrite-air and the data so collected are plotted as Fig. 5. Acceleration lengths calculated from the experimental data are listed in Table 3.

Increase in solid feed rate apparently increased the pressure drop per unit length, which is reasonable. The gas is forced to carry higher quantities of solids with increased solid feed rate. Further, it is noticed that from the data that, for a set of conditions, the accelerating length decreased with an increase in the solid loading rate. This can be explained by the fact that an enhanced solid flux reduces the void fraction, resulting there by in higher interstitial velocity, enhancing the drag on the particle and reducing the length of riser necessary to attain a stable flow condition.

3-1-4. Effect of material density on acceleration length

The effect of solid density on the pressure gradients at different

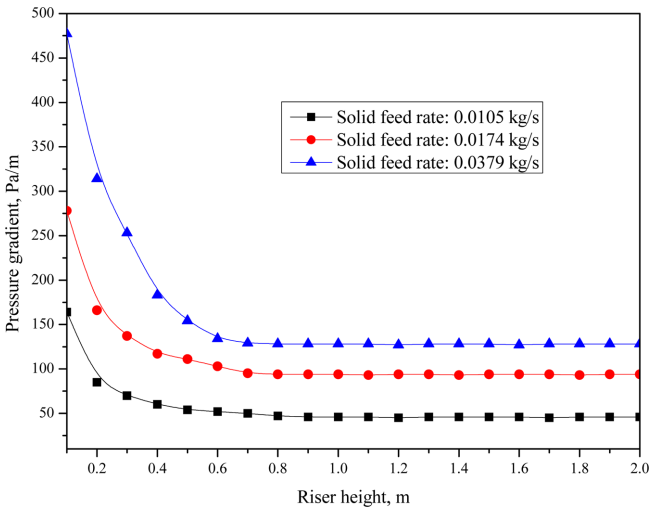

Fig. 5. Variation of pressure gradient with solid feed rate (Gas velocity: 10.61 m/s; Particle size: 98 μm).

Table 3. Variation of acceleration length with solid feed rate

Solid feed rate (w_s), kg/s	Acceleration length (L_A), m
0.0105	0.86
0.0174	0.79
0.0379	0.75

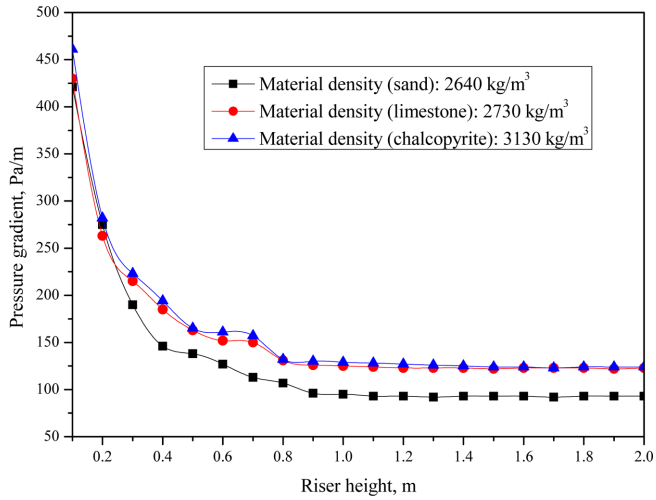

Fig. 6. Variation of pressure gradient with material density (System: Sand-Air, Limestone-Air, Chalcopyrite-Air; Gas velocity: 14.67 m/s; Solid feed rate: 0.0329 kg/s; Particle size: 480 μm).

Table 4. Variation of acceleration length with material density

Material density (ρ_p), kg/m^3	Acceleration length (L_A), m
2640 (sand)	1.09
2730 (limestone)	1.21
3130 (chalcopyrite)	1.52

riser heights is examined using three different systems – sand-air, limestone-air and chalcopyrite-air. The results are as shown in Fig. 6 and the corresponding acceleration lengths are listed in Table 4.

All three systems exhibited a uniform trend of lowering of pressure gradient exponentially as the riser height increases, reaching a steady horizontal level beyond a riser height of 0.9 m. Further, an increase in the material density enhanced the acceleration length with all other parameters remaining constant. This dependence can be explained by the fact that the higher the particle density, the higher will be the downward pull of gravity on these particles and hence, the higher will be the acceleration length to attain homogeneity overcoming the gravitational force.

Consolidated data, showing the pressure gradient per unit length against the different parameters considered, at lower, middle and top portion of the riser are as shown in Table 5.

The data clearly supports the hypothesis of acceleration length. Pressure gradient per unit length decreases in the lower half of the riser and remains steady in the upper half, regardless of levels of other parameters. The decrease in the ($\Delta P/\Delta L$) indicates the energy expended in dealing with the heterogeneity, i.e., the energy spent by the fluid to accelerate the solids and to help them attain a uniform velocity. Once this is achieved, the pressure gradient is maintaining a constant level.

3-1-5. Prediction of empirical model for acceleration length

A consolidated list of acceleration length obtained from the experimental study is provided as Table 6, to understand its dependence on the parameters studied and also to form the basis for development of

Table 5. Variation of pressure gradient

System: Chalcopyrite-air		Riser height (L), m		
		0.2	1.0	2.0
		Pressure gradient (ΔP/ΔL), Pa/m		
Air velocity (u_g), m/s	6.6	118	39	40
	7.9	192	46	46
	9.9	216	52	49
	14.53	224	57	51
Particle size (d_p), μm	98	362	102	102
	240	371	112	110
	480	382	114	111
	560	391	158	153
Solid feed rate (w_s), kg/sec	0.0105	85	46	46
	0.0174	166	94	94
	0.0379	314	128	128
Material density (ρ_p), kg/m^3	2640	275	95	93
	2730	279	125	123
	3130	282	129	124

a suitable correlation.

It is evident from the above table that an increase in the air velocity, increase in the particle size and increase in the particle density enhances the acceleration length, while an increase in solid feed rate decreases the acceleration length. All these factors - gas velocity (u_g), particle size (d_p), solid loading ratio (l_r), and material density (ρ_p) - need be considered while formulating a correlation for acceleration length (L_A). In addition, other physical properties of gas like gas density (ρ_g), gas viscosity (μ_g), acceleration due to gravity (g) and tube diameter (d_t) will also affect acceleration length, L_A.

Considering this, one may write

$$L_A = f(u_g, d_p, d_t, \rho_p, \rho_g, \mu_g, g, l_r) \tag{2}$$

Let the functional relationship be of the type,

$$L_A = (u_g)^{a1}.(d_p)^{a2}.(d_t)^{a3}.(\rho_p)^{a4}.(\rho_g)^{a5}.(\mu_g)^{a6}.(g)^{a7}.(w_s)^{a8}.(w_g)^{a9} \tag{3}$$

Expressing in terms of primary units of mass M, length L and time T and regrouping the variables, one gets

$$\frac{L_A}{d_t} = k\left(\frac{d_p}{d_t}\right)^a\left(\frac{w_s}{w_g}\right)^b\left(\frac{u_g\mu_g}{d_t^2 g\rho_g}\right)^c\left(\frac{\rho_p}{\rho_g}\right)^d \tag{4}$$

Through regression analysis of the experimental data, the constant k and exponents b, i, f and d are evaluated and the outcome is

$$\frac{L_A}{d_t} = 4.91902\left(\frac{d_p}{d_t}\right)^{0.10058}\left(\frac{w_s}{w_g}\right)^{-0.11691}\left(\frac{u_g\mu_g}{d_t^2 g\rho_g}\right)^{0.28574}\left(\frac{\rho_p}{\rho_g}\right)^{0.42484} \tag{5}$$

L_A values obtained from experiments and model equation are plotted in Fig. 7 and a reasonably good agreement between the two, especially in the trend is observed. A good concurrence in the magnitudes can also be noticed at most of the data points. Statistical analysis between the experimental and calculated (using correlation) values of the acceleration length is also made and a correlation coefficient of 0.95 obtained.

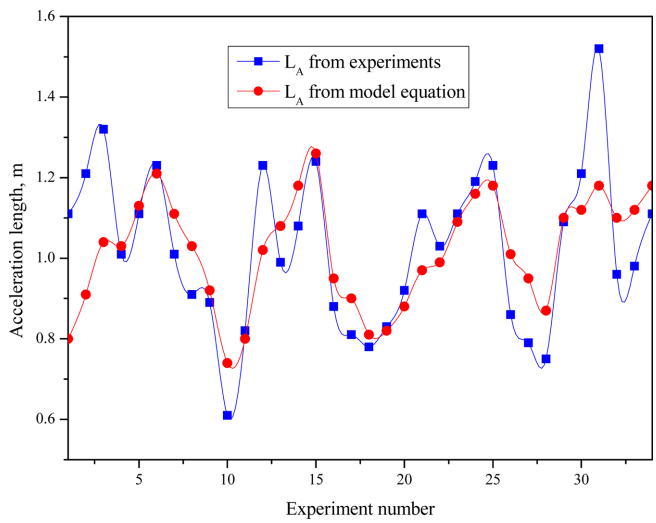

Fig. 7. Acceleration length (L_A) obtained from experiments and model equation.

Table 6. Values of acceleration length (L_A) obtained from experiments

System	Particle size, d_p, μm	Particle density, ρ_p, kg/m^3	Air velocity, u_g, m/s	Solid feed rate, w_s, kg/s	Air feed rate, w_g, kg/s	Acceleration length, L_A from experiments
Chalcopyrite-Air	98	3130	6.6	0.012	0.015	0.83
Chalcopyrite-Air	98	3130	7.9	0.012	0.018	0.92
Chalcopyrite-Air	98	3130	9.9	0.012	0.022	1.11
Chalcopyrite-Air	98	3130	14.53	0.036	0.033	1.03
Chalcopyrite-Air	240	3130	14.53	0.036	0.033	1.11
Chalcopyrite-Air	480	3130	14.53	0.036	0.033	1.19
Chalcopyrite-Air	560	3130	14.53	0.036	0.033	1.23
Chalcopyrite-Air	98	3130	10.61	0.010	0.024	0.86
Chalcopyrite-Air	98	3130	10.61	0.017	0.024	0.79
Chalcopyrite-Air	98	3130	10.61	0.037	0.024	0.75
Chalcopyrite-Air	480	3130	14.67	0.032	0.034	1.52
Chalcopyrite-Air	480	3130	14.67	0.032	0.034	1.11
Sand-Air	480	2640	14.67	0.0329	0.035	1.09
Limestone-Air	480	2730	14.67	0.0329	0.035	1.21
Chalcopyrite-Air	480	3130	14.67	0.0329	0.035	1.52

3-2. Heat transfer studies

It is mentioned in the preceding sections that an SP system works on the principle of fluid-to-particle heat transfer. In practice, the flue gas is fed through a series of cyclone separators, interconnected through riser pipes. Literature sources reveal that about 75% of the heat transfer takes place in the riser alone. As such, heat transfer in the riser plays a key role. Again, the rate of heat transfer within the riser may not be uniform all through. There can be faster rate of heat transfer in the lower section of the riser, which can diminish towards the end. It is, therefore, necessary to conduct both analytical and experimental studies on gas-to-solid heat transfer in the riser, particularly in the acceleration zone.

Using the gas and solid temperatures given in Tables 7 and 8, the rate of heat transfer and the heat transfer coefficient are estimated at different air and solid feed rates. This data is used to find the relation among Nu, Re_p and Pr. The equations employed are

$$\text{Rate of heat transfer, } q = \dot{m}C_p(\Delta T) \tag{6}$$

$$\text{Heat transfer coefficient, } h = \frac{q}{A(\Delta T)} \tag{7}$$

3-3. Correlation of Nusselt number

To fit the experimental data, a correlation of the following type has been developed, which is valid for higher ranges of solid concentration.

$$Nu = aRe_P^b Pr^c \tag{8}$$

$$\frac{hd_t}{k} = a\left(\frac{d_P\bar{v}\rho}{\mu}\right)^b\left(\frac{C_P\mu}{k}\right)^c \tag{9}$$

Through regression analysis of the experimental data, the constant a and exponents b and c were evaluated.

$$Nu = 0.40969(Re_P)^{0.99953}(Pr)^{0.03569} \tag{10}$$

Nusselt number values obtained from experiments and model equation are plotted in Fig. 8. The model is perhaps yielding the mean levels of the heat transfer coefficient, failing to indicate the cyclic increase and decrease. Statistical analysis between the experimental and calculated (using correlation) values of the Nusselt number yielded a correlation coefficient of 0.96.

Table 7. Variation of gas and solid temperatures along riser with solid feed rate (Average particle size: 240 μm; Air flow rate: 0.0351 kg/sec)

Riser height (m)	Solid feed rate (kg/sec)							
	0.0111		0.0143		0.0245		0.0346	
	t_g	t_p	t_g	t_p	t_g	t_p	t_g	t_p
0.0	188	37	188	36	186	38	188	37
0.2	174	79	177	62	172	58	166	52
0.4	169	92	164	73	158	66	156	58
0.6	166	101	158	81	154	72	144	63
0.8	162	114	157	93	147	80	140	70
1.0	159	123	153	99	143	85	134	73
1.2	156	127	148	106	139	92	132	75
1.4	157	129	147	109	138	97	130	77
1.6	152	132	144	114	135	104	128	79
1.8	150	135	143	118	133	109	124	81
2.0	148	138	141	123	131	113	121	83

t_g: Gas temperature in °C t_p: Solid temperature in °C

Table 8. Variation of gas and solid temperatures along riser with solid feed rate (Average particle size: 240 mm; Air flow rate: 0.0341 kg/sec)

Riser height (m)	Solid feed rate (kg/sec)							
	0.0121		0.0169		0.0232		0.0329	
	t_g	t_p	t_g	t_p	t_g	t_p	t_g	t_p
0.0	246	35	250	38	245	38	277	40
0.2	231	90	227	85	218	73	224	65
0.4	220	107	218	100	202	91	197	77
0.6	212	120	210	108	198	97	190	83
0.8	209	142	208	122	190	112	187	92
1.0	202	149	198	130	188	121	186	100
1.2	199	152	194	132	185	123	181	104
1.4	196	156	189	135	180	126	178	108
1.6	193	161	182	137	176	128	173	112
1.8	190	163	179	139	173	131	170	115
2.0	187	165	176	142	170	134	166	119

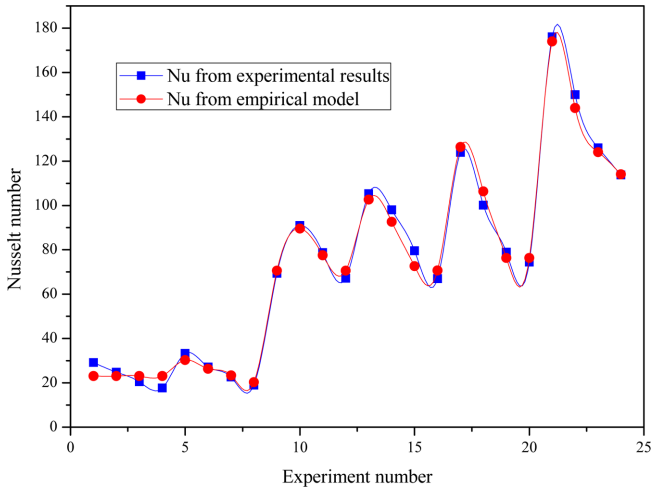

Fig. 8. Comparison of Nusselt number obtained from experiments and empirical model.

4. Conclusion

An experimental apparatus, along the lines of a riser used in the cement industry, was fabricated and exhaustive hydrodynamic studies were made by varying fluid velocity, solid feed rate, particle size and density. A mathematical model for the riser hydrodynamics was deduced using linear regression and the model equation was able to predict the acceleration (or mixing) length (L_A) of the riser. The correlation that is suggested for estimation of acceleration length goes as

$$\frac{L_A}{d_t} = 4.91902\left(\frac{d_p}{d_t}\right)^{0.10058}\left(\frac{w_s}{w_g}\right)^{-0.11691}\left(\frac{u_g\mu_g}{d_t^2 g\rho_g}\right)^{0.28574}\left(\frac{\rho_p}{\rho_g}\right)^{0.42484}$$

Instantaneous gas and particle temperature profiles were obtained experimentally. An empirical correlation was developed for Nusselt number as a function of Reynolds and Prandtl numbers using regression analysis which is valid for higher ranges of solid concentration. $Nu = 0.40969(Re_P)^{0.99953}(Pr)^{0.03569}$.

Nomenclature

A	: Heat transfer area [m^2]
c_p	: Specific heat [J/kg·°C]
d_p	: Particle diameter [m]
d_t	: Tube diameter [m]
g	: Acceleration due to gravity [m/s^2]
h	: Heat transfer coefficient [W/m^2·°C]
k	: Thermal conductivity [W/m·°C]
l_r	: Solid loading ratio
L	: Length of pipe [m]
L_a	: Acceleration length [m]
$\dot{m}$	: Mass flow rate [kg/s]
Nu	: Nusselt number
Pr	: Prandtl number
q	: Rate of heat transfer [W]
Re_P	: Particle Reynolds number
t_g	: Air temperature [°C]
t_p	: Particle temperature [°C]
u_g	: Air velocity [m/s]
w_g	: Air flow rate [kg/s]
w_s	: Solid feed rate [kg/s]
β	: Volume fraction of solids [1-ε]
ρ_p	: Solid density [kg/m^3]
ρ_g	: Air density [kg/m^3]
μ_g	: Air viscosity [kg/m·s]
ΔP/ΔL	: Pressure gradient per unit length of pipe [Pa/m]
ΔT	: Temperature difference [°C]

References

1. Marek, W., "Analysis of the Effects of Temperature and the Share of Solid and Gas Phases on the Process of Separation in a Cyclone Suspension Preheater," *Sep. Purif. Technol.*, **168**, 114-123(2016).
2. Yong, C., Faqi, Z. and Yaodong, W., "Experimental Analysis of the Solids Acceleration Region in a Circulating Fluidised Bed Riser," *Indian Chem. Eng.*, **57**(2), 136(2015).
3. Abdulkadir, M., Hernandez-Perez, V., Lowndes, I. S., Azzopardi, B. J. and Dzomeku, S., "Experimental Study of the Hydrodynamic Behavior of Slug Flow in a Vertical Riser," *Chem. Eng. Sci.*, **106**, 60-75(2014).
4. Huang Weixing and Zhu Jingxu, "An Experimental Investigation on Solid Acceleration Length in the Riser of a Long Circulating Fluidized Bed," *Chinese J. of Chem. Eng.*, **9**(1), 70-76(2001).
5. Xiao, Y. H., Wang, S. D., Yang, S. S., Zhao, K., Zeng, X. and Xu, X., "Solids Acceleration Length in a Cold Dense Transport Bed," *J. Thermal Sci.*, **21**(6), 533-538(2012).
6. Razzak, S. A., Barghi, S. and Zhu, J. X., "Axial Hydrodynamic Studies in a Gas–Liquid–Solid Circulating Fluidized Bed Riser," *Powder Technol.*, **199**, 77-86(2010).
7. Guangwen Xu, Kosuke Nomura, Nobuyoshi Nakagawa and Kunio Kato, "Hydrodynamic Dependence on Riser Diameter for Different Particles in Circulating Fluidized Beds," *Powder Technol.*, **113**(1-2), 80-87(2000).
8. Mitali Das, B., Meikap, C. and Saha, R. K., "A Critical Analysis of the Acceleration Length and Pressure Profile of Single-Particle Systems in a Circulating Fluidized Bed," *Asia-Pac. J. Chem. Eng.*, **3**, 560-571(2008).
9. Li, S., Wu, J. Y., Wang, R. Z. and Huangfu, Y., "Study of Heat and Mass Transfer in Integrated Thermal Management Controller (ITMC) Employed in Waste Heat Recovery Application," *Energy Convers. Manage.*, **48**, 3074-3083(2007).
10. Monazam, E. R. and Shadle, L. J., "Analysis of the Acceleration Region in a Circulating Fluidized Bed Riser Operating above Fast Fluidization Velocities," *J. Ind. Eng. Chem. Res.*, **47**, 8423-8429 (2008).
11. Huang, W. X., Zhu, J. X. and Parssinen, J. H., "Comprehensive Study on the Solids Acceleration Length in a Long CFB Riser," *J. Chem. Eng. Technol.*, **29**, 1197-1204(2006).
12. Pandey, K. M. and Ray, M., "Experimental Studies on Hydrody-

namics of a Cyclone Separator Employed in a Circulating Fluidized Bed," *Int. J. Chem. Eng. Appl*., **1**(2), 123-131(2010).
13. Yang, Y. L., Jin, Y., Yu, Z. Q., Wang, Z. W. and Bai, D. R., "The Particle Velocity Distribution in a Riser of Dilute Circulating Fluidized Bed," *J. Chem. Ind. Eng*., **2**, 182-191(1991).
14. Kalita, P., Saha, U. K. and Mahanta, P., "Parametric Study on the Hydrodynamics and Heat Transfer along the Riser of a Pressurized Circulating Fluidized Bed Unit," *Exp. Therm. Fluid Sci*., **44**, 620-630(2013).
15. Blasetti, A. and De Lasa, H., "Heat-Transfer Prediction in the Riser of a Novel Fluidized Catalytic Cracking Unit," *Ind. Eng. Chem. Res*., **40**, 4623-4632(2001).
16. Bai, D. R., Jin Yong and Yu Zhiqing, "The Particle Acceleration and the Interaction Between Gas and Solids in the Riser of Circulating Fluidized Beds," *J. Chem. React. Eng. Technol*., **3**, 260-270(1991).
17. Ferschneider, G. and Mège, P., "Dilute Gas-Solid Flow in a Riser," *Chem. Eng. J.*, **87**(1), 41-48(2002).
18. Kaczmarzyk, G., Bandroski, J., "Gas-Solid Heat Transfer Coefficients in Vertical Pneumatic Transport," *Int. Chem. Engg*., **20**, 98-110(1980).
19. Bai, D. R., Jin, Y. and Yu, Z.Q., "The Length of Particle Acceleration Region in Fast Fluidized Beds," *J. Chem. React. Eng. Technol*., **6**, 34-39(1990).
20. Sharlovskaya, M. S., "Investigation of Heat Transfer in Fluidized Bed by Using the Quasi-Stationary Method (in Russian)," *Reports of Siberian Branch of AS SSSR*, **7**, 62-74(1958).
21. Watanabe, T., Yong, C., Hasatani, M., Yushen, X., and Naruse, I., "Gas to Particle Heat Transfer in Fast Fluidized Bed," Circulating Fluidized Bed Technology III, Oxford Pergamon Press, 283-287(1991).
22. Reddy, B. V. and Nag, P. K., "Effect of Riser Exit Geometry on Bed Hydrodynamics and Heat Transfer in a Circulating Fluidized Bed Riser Column," *Int. J. Energy Res*., **25**(1), 1-8(2001).